

*Transactions, SMiRT-25*  
Charlotte, NC, USA, August 4-9, 2019  
Division II

## **USING LOCAL APPROACHES TO FRACTURE TO QUANTIFY THE LOCAL CONDITIONS DURING THE DUCTILE-TO-BRITTLE TRANSITION IN FERRITIC STEELS**

**Maria S Yankova<sup>1</sup>, Andrey P Jivkov<sup>2</sup>, Rajesh Patel<sup>3</sup>, Andrew H Sherry<sup>4</sup>**

<sup>1</sup> Post-doctoral research associate, School of MACE, University of Manchester, Manchester, UK.  
([maria.yankova@manchester.ac.uk](mailto:maria.yankova@manchester.ac.uk))

<sup>2</sup> Professor of Solid Mechanics, School of MACE, University of Manchester, Manchester, UK.

<sup>3</sup> Project Manager, National Nuclear Laboratory, Warrington, UK

<sup>4</sup> Professor of Materials Performance, School of Materials, University of Manchester, Manchester and Chief Scientist, National Nuclear Laboratory, Warrington, UK.

### **ABSTRACT**

Ferritic steels, which are typically used for critical reactor components, including reactor pressure vessels (RPV), exhibit a ductile-to-brittle transition. The fracture process has been linked to the interaction between matrix plasticity and second phase particles. Under high-enough loads, a competition exists between particles rupturing to form micro-cracks and particles decohering to form micro-voids, which are prerequisites for cleavage and ductile fracture, respectively. Currently, there is no sufficiently adequate model that can predict the competition between these two failure mechanisms and hence fracture toughness values in ferritic steels. In this work, failure probability has been estimated using a local approach to cleavage fracture incorporating the statistics of micro-cracks. It is shown that changes in the deformation material properties are not enough to capture the significant changes in fracture toughness. Instead, a correction to the fraction of particles converted to eligible for cleavage micro-cracks is proposed. The method is developed for the RPV steel 22NiMoCr37 and using experimental data for a standard compact tension C(T) specimen. The proposed approach offers more accurate calculations of fracture toughness in the ductile-to-brittle transition regime using only decoupled models, which is attractive for engineering practice.

### **INTRODUCTION**

Ferritic steels are widely used for reactor pressure vessels and other pressure boundary components in nuclear reactors due to their high strength and good fracture toughness properties. However, like other body-centred-cubic metals, they exhibit a ductile-to-brittle transition (DBT), which leads to an increased probability of cleavage fracture with decreasing temperature. In unirradiated material, the transition usually occurs approximately at or below room temperature, as seen in a report by IAEA (1992). However, environmental factors such as irradiation or presence of embrittling species due to material ageing, can alter the steel properties in service and progressively shift the brittle-to-ductile transition temperature, e.g. see Steele (1975). In addition to this, a large scatter in the measured fracture toughness is observed – a consequence of the stochastic nature of the cleavage fracture process determined by the material's microstructure. The random distribution of second phase particles, such as carbides and sulphide inclusions, have been shown to have a critical role – under high-enough loads, a competition between particles rupturing to form micro-cracks and particles decohering to form micro-voids takes place, which are prerequisites for respectively cleavage and ductile fracture. At sufficiently low temperatures, solely

cleavage is observed, and as temperature increases, the ductile damage occurs within an increasing volume ahead of the crack, until at upper-shelf temperatures, cleavage does not occur.

Local approaches to fracture (LAF) model cleavage as a probabilistic event based on local fracture criteria for an unstable critical Griffith-like microcrack in a volume element and consider the probability density distribution of these microcracks. Thus, these approaches were developed as a mechanistic micromechanical method for modelling cleavage as an alternative to highly conservative global approaches, based on a single parameter such as  $K_{IC}$ ,  $J_{IC}$  or CTOD. Many studies have applied LAF to predict fracture in ferritic steels, but currently there is no sufficiently adequate model, which correctly reproduce the competition between cleavage and ductile damage in the DBT regime. The existing local approaches to cleavage usually correctly predict the lower-shelf toughness, but with increasing temperature toughness is increasingly underestimated. The current work utilises a cleavage fracture model, firstly introduced by the Beremin group (1983), to estimate failure probability. A temperature-dependent correction to the cleavage initiators density is compared to the original model, which shows that micro-mechanical processes must be affecting the fraction of eligible micro-cracks as temperature changes.

## METHODOLOGY

### *Material Properties*

The pressure vessel steel 22NiMoCr37, also known as Euro Reference Material A, was considered for the development of the model. The fracture toughness properties within the lower shelf and DBT are available from the Euro fracture dataset in Heerens et al. (2002). Data for a standard 1T compact tension, C(T) specimen with width  $W = 50$  mm, thickness  $B = 25$  mm, and crack length  $a = 25$  mm, at four temperatures:  $-154^\circ\text{C}$ ,  $-91^\circ\text{C}$ ,  $-60^\circ\text{C}$ ,  $-40^\circ\text{C}$ , are used for the analysis in the present work. The experimental fracture toughness values,  $J_c$ , have been sorted in ascending order, so that  $J_c^k \leq J_c^{k+1}$  for  $k = 1, \dots, N - 1$ , where  $k$  is the ranking number and  $N$  is the total number of measurements. The cumulative probability of cleavage fracture at each data point is provided by the median ranking  $F(J_c^i) = (i - 0.3)/(N + 0.4)$ . The cumulative probabilities for the four temperatures are shown in Figure 5 (a-d). These are compared with a Weibull fit using the maximum likelihood (ML) method.

Deformation properties of the material at the considered temperatures are given in Table 1, where  $E$  is the Young's modulus,  $\sigma_0$  is the proportionality stress,  $\sigma_{UTS}$  is the ultimate tensile strength and  $n$  is the power law hardening exponent (see James et al. (2014)).  $\sigma_u$  and  $\varepsilon_u$  correspond to the true stress and strain, at which  $\sigma_{UTS}$  occurs. The Poisson's ratio  $\nu$  was found to be independent of temperature with a value of 0.3. Finally, a flow stress,  $\sigma_f$ , is defined as a weighted average between  $\sigma_0$  and  $\sigma_u$  by the following computation ( $\varepsilon_0 = \sigma_0/E$ ):

$$\sigma_f = \frac{1}{\varepsilon_u - \varepsilon_0} \int_{\sigma_0}^{\sigma_u} \sigma \, d\varepsilon. \quad (1)$$

Table 1. Deformation properties of 22NiMoCr37 at the considered temperatures.

$T_i$ ( $^\circ\text{C}$ )	$E$ (MPa)	$\sigma_0$ (MPa)	$\sigma_{UTS}$ (MPa)	$n$	$\sigma_u$ (MPa)	$\sigma_f$ (MPa)
-154	219860	768.3	856.3	16.812	908.6	848.5
-91	214190	594.9	727.1	11.978	790.5	723.6
-60	211400	544.7	686.5	11.030	751.5	683.5
-40	209600	520.4	665.8	10.596	731.2	663.0

### Finite Element Analysis

Three-dimensional models of a quarter standard compact tension specimen, 1T C(T), with finite crack tip radii were used in the large strain finite element analyses, as implemented in Abaqus (version 2017). The crack tip radii  $r_i = 1, 10, 15$  and  $30 \mu\text{m}$  for the corresponding  $T_i$ , were chosen proportional to the maximum crack tip opening displacement obtained using a boundary layer model with sharp crack tips. Figure 1 (a) shows as an example the quarter-C(T) model with a  $30\text{-}\mu\text{m}$  radius, where the applied symmetry conditions are denoted. To speed-up convergence, the model was loaded by applying displacement increments on the edge of a purely elastic wedge, which was used as a model for the experimental loading pins, typically made of a high yield strength maraging steel (see ASTM (2018)). Figure 1 (b) shows the focused mesh near the crack tip – the ninety-degree segment was divided in six equal-angle segments, and the element thickness ahead of the crack front increases with the thickness of the first element set to between two and three times the crack tip radius. Furthermore, a higher density mesh was used near the outer free surface of the specimen with 20 variable thickness layers defined over the half-thickness in order to capture stronger variations in the stress and strain distribution. The  $J$  integral is obtained at a contour in the same position of the specimen for all temperature cases. Computationally, the material is modelled as elastic-plastic and the flow properties were provided in Abaqus in a tabular form. Figure 2 shows the normalised maximum principal stress and the equivalent plastic strain fields ahead of the crack tip.

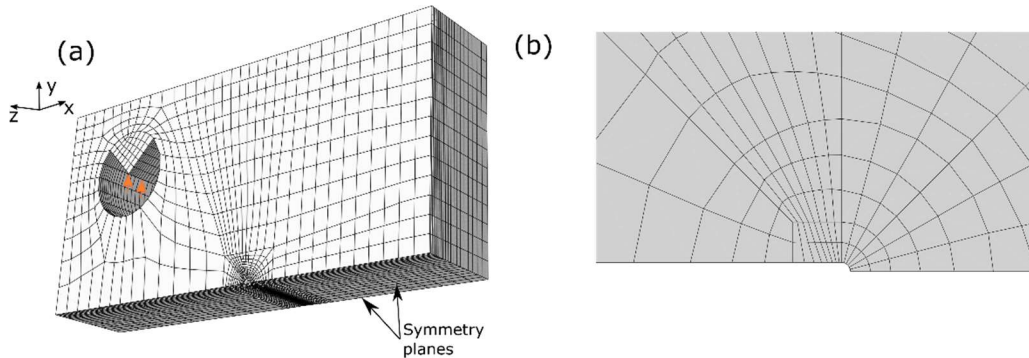


Figure 1. Finite element 3D quarter 1T C(T) model (a) and high-density mesh around the crack tip (b).

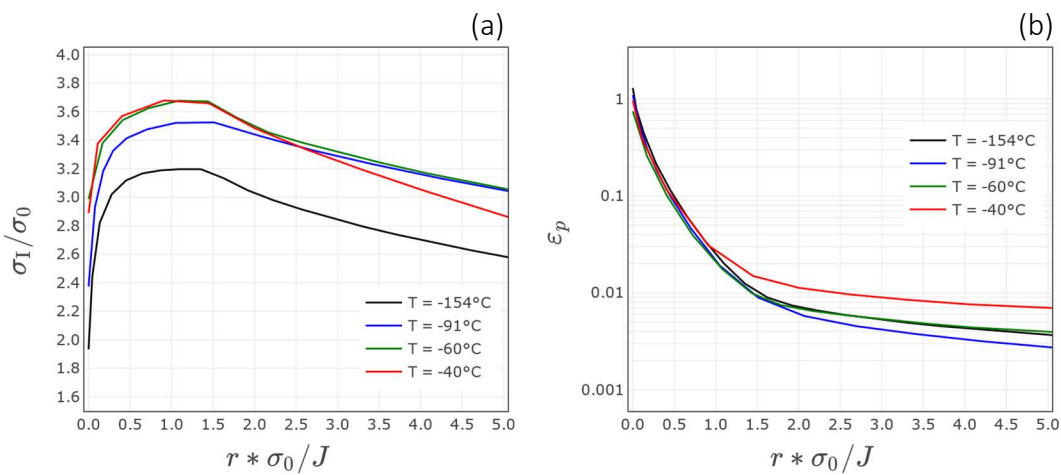


Figure 2. Normalised maximum principal stress (a) and equivalent plastic strain (b) for the 1T C(T) models at all temperatures.

### ***Statistical Cleavage Fracture Model***

Cleavage fracture in ferritic steels initiates from elastic-brittle second-phase particles in the material, for example carbides or sulphide inclusions, which rupture under high tensile stress of the plastically deforming surrounding matrix – a process referred to as plastic overload. The statistical nature of cleavage originates from the spatial random distribution of second-phase particles of variable sizes, which are converted into micro-cracks of variable sizes. Depending on the local mechanical fields, a particle of a given size may: (1) remain intact, i.e. continue deforming with the matrix; (2) detach from the matrix forming a void, which grows with further plastic straining; (3) break, forming a micro-crack, which blunts due to local conditions and continues as in (2); or (4) break, forming a micro-crack, which can propagate to cleave the component. Hence, it is important to distinguish between particles, voids/micro-cracks not eligible for cleavage initiation, and micro-cracks eligible for cleavage.

The existing probabilistic models assume cleavage to be approximated by a Poisson process, which is a model of events that happen completely at random, for example see Kingman (2002). There are three characteristics of the Poisson process: (1) failures of non-overlapping volumes are completely independent; (2) the probability of failure of a volume element  $\delta V$  is proportional to its volume; (3) the probability of more than one failure in  $\delta V$  is assumed zero. Based on the first assumption, weakest-link theory states that the survival probability of the solid is equal to the product of survival probabilities of all volume elements. If the fracture process zone ahead of the crack tip is divided into statistically independent and uniformly stressed unit volumes,  $\delta V$ , which contain uniformly distributed micro-cracks with probability density,  $f_c(a)$ , the probability of failure of a volume element  $\delta P_f$ , and that of the solid  $P_f$  are expressed as:

$$\delta P_f = \mu_c \delta V = \left( \frac{1}{V_0} \int_{a_c}^{\infty} f_c(a) da \right) \delta V, \quad P_f = 1 - \exp(- \int_V \mu_c dV), \quad (2)$$

where  $\mu_c$  is the number density of unstable micro-cracks and  $a_c$  represent a critical micro-flaw size. The reference volume  $V_0$  was approximated as the volume of a spherical grain with a 10  $\mu\text{m}$  radius. Here, we included volume elements with a plastic strain larger than 0.01%.

Calculations of a component's probability of cleavage fracture by this equation will be as realistic as is the assessment of the number density of cleavage initiators,  $\mu_c$ , i.e. how particular mechanical fields determine the critical micro-crack size,  $a_c$ , and the probability density of eligible micro-crack sizes,  $f_c(a)$ . This is a challenging task due to limited experimental data. Experimental works demonstrate a clear link between the level of plastic strain and the number of micro-cracks formed by rupturing particles, but do not provide sufficient evidence for determining  $f_c(a)$  and particularly its dependence on temperature. This lack of knowledge makes it necessary to test different possibilities for the functional form of  $f_c(a)$ . Considering firstly that  $f_c(a)$  should be zero in the absence of plastic strains, the Beremin group's original suggestion was that within the plastic zone ahead of a macroscopic crack  $f_c(a)$  was approximated by a power law  $(a_0/a)^\beta$  representing the tail of the particle size distribution. Here,  $a_0$  and  $\beta$  are the scale and shape parameters, respectively. This is equivalent to the assumption that all particles in the tail are converted into eligible micro-cracks with the onset of plasticity. If it is assumed that the size distribution of eligible micro-cracks has the same shape as the size distribution of particles, i.e. the same  $\beta$  and  $c(\epsilon_p)$  represents the fraction of particles converted into eligible micro-cracks assuming dependence on the plastic strains  $\epsilon_p$ , then

$$f_c(a) = c(\epsilon_p)(a_0/a)^\beta. \quad (3)$$

In the original Beremin model  $c(\epsilon_p) = H(\epsilon_p)$ , where  $H(\epsilon_p)$  is the Heaviside step function. We compare that model with another type of correction, firstly proposed by Ruggieri et al. (2015), which is given by

$$c(\varepsilon_p) = 1 - \exp[-\lambda(T)\varepsilon_p], \quad (4)$$

where  $\lambda$  is a material parameter, which is a function of temperature.

The critical micro-crack size is calculated from a criterion for unstable growth, e.g. for a penny-shaped crack formed by rupture of a particle the critical size is

$$a_c = \frac{\pi E \gamma}{2(1-\nu^2)\sigma_1^2}, \quad (5)$$

where  $E$  and  $\nu$  are, respectively, the elastic modulus and Poisson's ratio of the steel,  $\sigma_1$  is the maximum principal stress, and  $\gamma$  is a measure of fracture energy. The free surface energy of the steel,  $\gamma_s$ , is assumed to be a good approximation for the fracture energy in the case of limited plasticity. Using Equations (3)-(5) and integrating leads to an expression for the number density of cleavage initiators as a power law of the effective stress

$$\mu_c = \frac{1}{V_0} c(\varepsilon_p) \left(\frac{\sigma_1}{\sigma_u}\right)^m, \quad (6)$$

where the shape parameter is  $m = 2\beta - 2$ , and the scale parameter  $\sigma_u$  collects the elastic properties, the constant surface energy, and the scale of the power law. Then, substitution of Equation (6) into Equation (2) yields a two-parameter Weibull distribution, Equation (7), of an integral stress parameter,  $\sigma_w$ , known as Weibull stress, Equation (7). The Weibull stress is considered as a crack driving force for cleavage fracture.

$$P_f(\sigma_w) = 1 - \exp\left[-\left(\frac{\sigma_w}{\sigma_u}\right)^m\right]. \quad (7)$$

$$\sigma_w = \left[\frac{1}{V_0} \int_V c(\varepsilon_p) \sigma_1^m dV\right]^{1/m}. \quad (8)$$

## RESULTS AND DISCUSSION

Figure 3 shows how the Weibull stress, scaled with the flow stress at the corresponding temperature, varies for a range of values of the Weibull shape parameter. In (a) the original Beremin model with the Heaviside step function is applied – the Weibull stress increases with decreasing temperature. And, although as the shape parameter is increased, that difference decreases, there is no shape parameter within reasonable limits, for which the Weibull stress at different temperatures can be made equal. This observation suggests that the mechanical fields alone cannot provide sufficient information for a model to be able to predict the change of toughness with temperature. As seen in Figure 2, there is no sufficiently great difference in the mechanical fields ahead of the crack tip with changing temperature. On the other hand, if a correction is applied based on Equation 4, the scaled Weibull stress curves as a function of  $m$  appear to be very close to coinciding, as seen in Figure 1(b). The  $\lambda$  parameter is dependent on temperature through the micro-mechanisms that are active at a given temperature. There is a significant drop of four orders of magnitude between the fitted value of  $\lambda$  at the lowest and at the highest temperature, which corresponds to a large decrease in the fraction of particles converted into eligible micro-cracks as the temperature increases. The number of micro-cracks appears constant across temperatures, however, spread across a different volume of material.

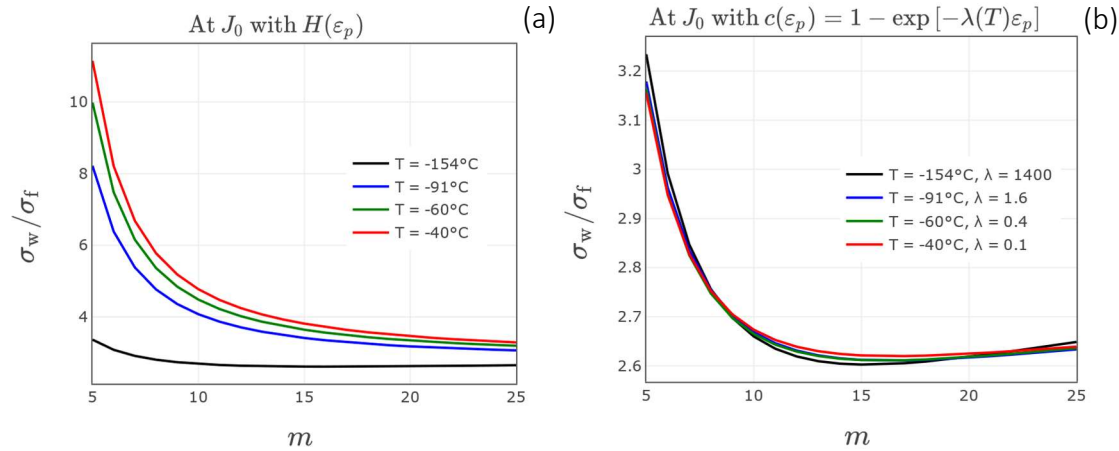


Figure 3. Variation of the scaled Weibull stress with shape parameter for different temperatures using two types of correction: the Heaviside step function (a), and an exponential function as shown in Equation 4, where the  $\lambda$  parameter is a function of temperature (b).

Next, it is demonstrated how the probability of fracture can be predicted at any temperature, given a series of fracture toughness tests at a certain temperature. Figure 4 shows the Weibull stress as a function of  $J$  for the four temperatures. The Weibull shape parameter was set to 5.4, which corresponds to the experimentally measured distribution of particle sizes. With a dotted line is denoted the value of the Weibull stress at the characteristic  $J_0$  using the experimental data at  $T = -91^\circ\text{C}$ . The points where this line crosses the Weibull curves correspond to the  $J_0$  value, since the scaled Weibull stress is set to be independent of temperature at  $J_0$ . The corresponding characteristic  $J_0$  at the other temperatures as calculated based on the experimental data available and the prediction from Figure 4 are shown in Table 2. For all three temperatures, the predicted values were found to be in good agreement with a slight underestimation of the experimental values. Therefore, the proposed calibration method only requires fracture toughness tests at a selected temperature, combined with deformation properties for any other temperature of interest. Weibull stresses can then be computed and  $J_0$  estimated using an FE model and numerical analysis.

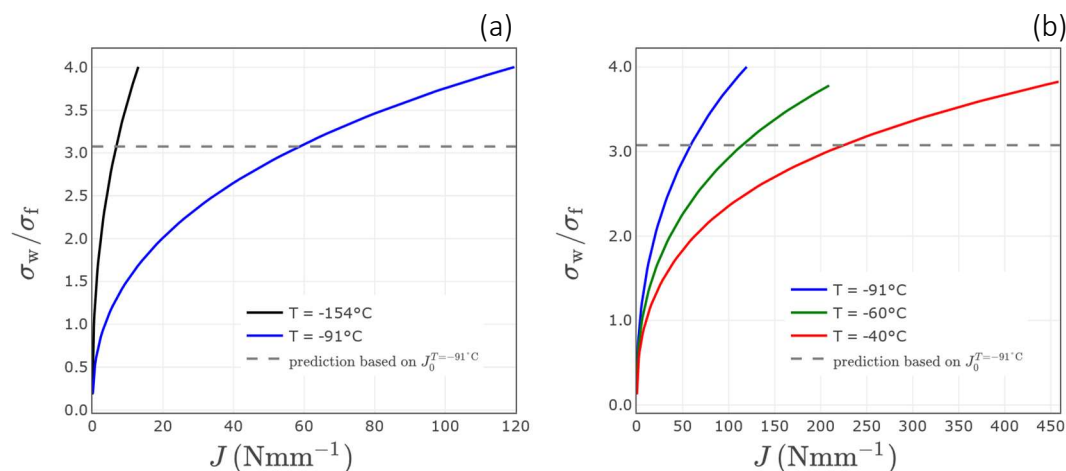


Figure 4. Variation of the ratio of Weibull stress over flow stress with the fracture toughness  $J$  calculated with a Weibull shape parameter  $m = 5.4$  and a scale parameter  $\sigma_u = 2.97\sigma_f$  for the four temperatures. A dotted line represents the value of the Weibull stress at the characteristic fracture toughness  $J_0$  at  $T = -91$

°C based on a Weibull distribution fit to the fracture toughness data using the maximum likelihood method (see Figure 5).

Table 2. Comparison between characteristic fracture toughness  $J_0$  calculated based on a Weibull distribution fit to the experimental data using the maximum likelihood method, and predicted using the proposed method based on the fracture toughness experimental data at  $T = -91$  °C.

$T$ (°C)	$J_0^{\text{EXP}}$ (Nmm <sup>-1</sup> )	$J_0^{\text{SIM}}$ (Nmm <sup>-1</sup> )
154	7.7	6.6
-91	57.6	–
-60	112.8	107.4
-40	235.3	216.9

The data at  $T = -91$  °C was further used to fit a two-parameter Weibull distribution and calibrate a value for  $\sigma_u = 2.97\sigma_f$ . It was then possible to estimate the cumulative probability functions of the experimentally measured  $J_c$  for each of the other temperatures, as seen in Figure 5. The current model provides a good estimation of the fracture toughness probability distribution, particularly at high fracture toughness values. Across all temperatures, there is a small underestimation of the experimental results, which is preferable to an overestimation.

## CONCLUSION

A local approach to cleavage fracture utilising the statistics of micro-cracks combined with finite element analysis were applied in calculating the failure probability of a ferritic steel in the ductile-to-brittle regime. The findings of the study can be summarised as follows:

- It was demonstrated that the change in the material deformation properties with change in temperature is insufficient to capture the change in fracture toughness across temperatures.
- An exponential correction dependent on the plastic strains and a material property, which depends on temperature, to the density of micro-cracks eligible for cleavage was proposed.
- The developed procedure for probability of cleavage estimation would only require experimental fracture toughness tests at a given temperature, and deformation properties at any other temperature.
- A very good agreement was shown between the predicted and experimentally measured characteristic fracture toughness as well as the predicted and experimentally fitted probability distributions.
- Future work will focus on investigating the reason behind the observed exponential temperature dependence of eligible micro-cracks density.

## ACKNOWLEDGEMENTS

The authors gratefully acknowledge funding from the National Nuclear Laboratory and Électricité de France. Furthermore, A. P. Jivkov acknowledges the financial support of the Engineering and Physical Sciences Research Council UK (EPSRC) via grant EP/N026136/1.

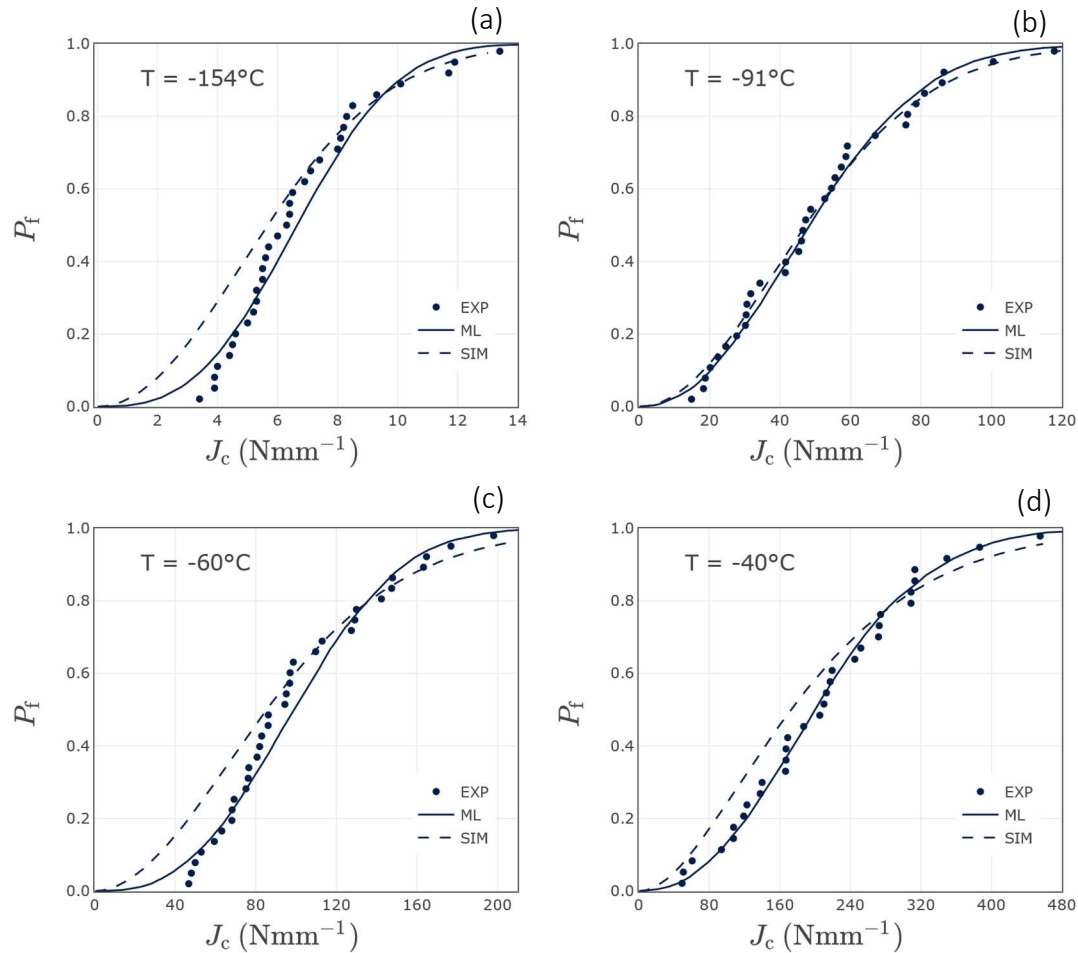


Figure 5. Cumulative probability function of experimentally measured  $J_c$  and Weibull fit as predicted by the proposed method.

## REFERENCES

- ASTM. (2018). E399-17 “Standard Test Method for Linear-Elastic Plane-Strain Fracture Toughness  $K_{Ic}$  of Metallic Materials 1”.
- Beremin, F. M. (1983). “A local criterion for cleavage fracture of a nuclear pressure vessel steel”. *Metallurgical Transactions A*, 14(11), 2277–2287.
- Heerens, J., & Hellmann, D. (2002). “Development of the Euro fracture toughness dataset”. *Engineering Fracture Mechanics*, 69(4), 421–449.
- International Atomic Energy Agency. (1992). “Reactor pressure vessel embrittlement”. *Report of the IAEA extra budgetary programme on the safety of WWER-440 model 230 nuclear power plants*.
- James, P. M., Ford, M., & Jivkov, A. P. (2014). “A novel particle failure criterion for cleavage fracture modelling allowing measured brittle particle distributions”. *Engineering Fracture Mechanics*, 121–122, 98–115.
- Kingman, J. F. C. (2002). *Poisson processes*. New York: Oxford Univ. Press.
- Ruggieri, C., Savioli, R., Dodds Jr., R. H. (2015). “An engineering methodology for constraint corrections of elastic-plastic fracture toughness – Part II: Effects of specimen geometry and plastic strain on cleavage fracture predictions”. *Engineering Fracture Mechanics*. 146, 185-209.
- Steele, L. E. (1975). *Neutron Irradiation Embrittlement of Reactor Pressure Vessel Steels*. Vienna.